IOP Conf. Series: Journal of Physics: Conf. Series **1461** (2020) 012028 doi:10.1088/1742-6596/1461/1/012028

Quantum light sources based on deterministic microlenses structures with (111) In(Ga)As and AlInAs QDs.

I A Derebezov[1], V A Haisler[1], A V Haisler[1], D V Dmitriev[1], A I Toropov[1], S Rodt[2], M von Helversen[2], C de la Haye[2], S Bounouar[2], S Reitzenstein[2]

[1] Rzhanov Institute of Semiconductor Physics, Siberian Branch, Russian Academy of Sciences, pr. Academika Lavrent'eva 13, Novosibirsk, 630090 Russia
[2] Technische Universitaet Berlin, Hardenbergstrasse 36, Berlin, D-10623 Germany

Abstract

The results of the development and implementation of a single photon source based on a bottom semiconductor Bragg reflector, top deterministic GaAs microlens structures and a single (111) In(Ga)As QD are presented. The structure of the microcavity ensures effective pumping of a single (111) In(Ga)As QD and high emission output efficiency, a clear single – photon emission was detected with a second – order correlation function at zero delay $g^{(2)}(0) = 0.07$. A system of QD's on the basis of $Al_XIn_{1-X}As/Al_YGa_{1-Y}As$ solid solutions has been studied. The usage of broadband $Al_XIn_{1-X}As$ solid solutions as the basis of quantum dots makes it possible to expand considerably the spectral emission range into the short-wave region, including the wavelength region near 770 nm being of interest for the design of aerospace systems of quantum cryptography. The optical characteristics of single $Al_XIn_{1-X}As$ quantum dots grown according to the Stranski–Krastanov mechanism are studied by the cryogenic microphotoluminescence method.

1. INTRODUCTION

Non-classical light sources emitting single photons or entangled photon pairs on demand constitute key building blocks towards the realization of advanced quantum communication networks [1–5]. In recent years, single self assembled quantum dots (QDs) integrated into photonic microstructures have turned out to be very promising candidates for realizing such quantum-light sources [6–10]. Single QDs can emit of entangled photon pairs in the process of cascade recombination of biexcitons (XX) and excitons (X) in the case where exciton states are energy degenerated or their splitting ΔE_{FS} does not exceed the natural width of the exciton levels $\Gamma_X = \hbar/\tau_X$, where τ_X is the lifetime of an exciton. In this case, the study touches upon the entangled photon pair. In real QDs grown on substrates with orientation (001), the splitting of exciton states ΔE_{FS} usually exceeds the natural width of the exciton levels Γ_X many times, which is due to deviation of the QD form from a perfect one and the presence of a piezopotential induced by embedded mechanical stresses. This is the main obstacle in developing QD based emitters of entangled photon pairs. One of the solutions of this problem is to use QDs grown on substrates with orientation (111). In this case, we have QDs of the symmetry C_{3V}, in which, according to [11], the splitting of exciton states ΔE_{FS} can be suppressed to zero values. The system of InAs/GaAs quantum dots with the unique wide spectral range reaching ~400 nm including the first and second telecommunication standards (~0.9 and 1.3 μm, respectively) is the most studied to date. The single-photon emission and emission of pairs of entangled photons at wavelengths near the first telecommunication standard were

demonstrated using single InAs QDs [12, 13]. The expansion of the spectral range of quantum dots into the short-wavelength region is of interest for studying physics of new low-dimensional semiconductor systems and creating emission sources for systems of atmospheric or aerospace quantum cryptography. The wavelength region near 770 nm [14], where the sensitivity of silicon photodetectors is maximal, and the absorption of the atmospheric layer and fluctuations of the local refractive index are minimal, which is necessary for the maintenance of the photon polarization, is optimal for these systems.

In this work, we realize a single photon source on (111)B GaAs substrate based on bottom DBR, a deterministically integrated single-QD and top microlens structure. Probing the photon statistics of the emission of a single QD-state we demonstrate single-photon emission of the QD microlens with $g^{(2)}(0) = 0.07$. In additional we consider mechanisms of the formation and the optical characteristics of quantum dots on the basis of $Al_xIn_{1-x}As/Al_yGa_{1-y}As$ ternary solid solutions. The optical characteristics of single $Al_xIn_{1-x}As/Al_yGa_{1-y}As$ QD's grown according to the Stranski–Krastanov mechanism were studied for the first time by the cryogenic microphotoluminescence method. Hanbury Brown and Twiss experiment has been carried out to measure the photon statistics. Photon correlation function demonstrates a clear photon antibunching effect, what is a direct evidence of a single photon emission by $Al_xIn_{1-x}As$ a single quantum dot.

2. SAMPLE PREPARATION

$Al_xIn_{1-x}As/Al_yGa_{1-y}As$ structures were grown on GaAs(001) substrates by molecular-beam epitaxy (MBE) system Riber – C21. The full structure containes two 40-nm thick $Al_{0.7}Ga_{0.3}As$ layers inhibiting the diffusion of photoexcited charge carriers and a 200-nm-thick $Al_yGa_{1-y}As$ layer sandwiched between the abovementioned two layers. In the middle of the 200-nm thick $Al_yGa_{1-y}As$ layer absorbing the major part of the laser excitation power, there was a layer of $Al_xIn_{1-x}As$ QDs. We studied $Al_xIn_{1-x}As$ QDs whose composition parameter was in the range of x= 0–0.3 with a step of 0.05. In this case, the composition of the $Al_yGa_{1-y}As$ layers was specified to provide the relation $y \approx 1.7x$. The layer of $Al_xIn_{1-x}As$ QDs was grown by the Stranski–Krastanov mechanism at the temperature T= 505°C. On the $Al_yGa_{1-y}As$ surface, an $Al_xIn_{1-x}As$ layer was grown to the critical thickness (~2 single layers (SL)). As the critical thickness was attained, an array of selfassembled $Al_xIn_{1-x}As$ QDs began to emerge. The growth rate of the $Al_xIn_{1-x}As$ layer was 0.045 SL s^{-1}. The transition from the two-dimensional mechanism of growth to the three-dimensional mechanism was monitored by the high-energy electron-diffraction method. As the critical thickness was attained, the process of growth of $Al_xIn_{1-x}As$ stopped, and in the time τ_{GI}, an array of $Al_xIn_{1-x}As$ QDs was formed by the Ostwald mechanism [15-17], after which the $Al_xIn_{1-x}As$ layer was overgrown by $Al_yGa_{1-y}As$. The time of growth interruption was τ_{GI}= 10 s.

The structure containing (111)-oriented In(Ga)As QDs was synthesized by MBE on 2°-misoriented n+ GaAs(111)B substrate. The initial structure of the microcavity consists of a semiconductor distributed Bragg reflector (DBR) and a GaAs layer containing an (111) InGaAs QD layer.. The DBR contains 23 periods of alternating quarter-wave layers of GaAs and $Al_{0.9}Ga_{0.1}As$, which ensures the high reflection coefficient ($R \geq 0.99$) at the operating wavelengths near 930 nm. The GaAs layer grown on the DBR surface has thickness 2λ. There is a QD layer located inside this layer at distance λ/2 from the DBR. There is also the 10-nm thick $Al_{0.4}Ga_{0.6}As$ layer located inside the GaAs layer at distance λ from the DBR and preventing the diffusion of photoexcited carriers to the structural surface. The GaAs microlens structures were formed by a device created on an electron microscope and combining the capabilities of measuring the cryogenic cathode-luminescence (CL) spectra with high spatial resolution and carrying out electron lithography. The first step comes down to determining the lateral coordinates of suitable single QDs, which are of interest in developing non-classical light sources. For this purpose, the electron beam is used to scan the structural region and measure the cryogenic CL spectra. The next step is three-dimensional electron lithography carried out in order to form a lens-shaped resistive mask placed according to certain coordinates of the single QD. To perform this procedure, the microscope electron beam with a carefully controlled power circumscribes the concentric circles whose center is determined by the single QD coordinates. The removal of the unexposed resist is followed by plasma-chemical etching of the structure. As the etching rates of the lens-shaped resistive mask and GaAs are approximately equal, the etching causes the shape of the semiconductor material to become identical to that of the mask. As a result, there is a GaAs microlens of a controlled size that is formed on the structure surface and located over the chosen single QD. The lens diameter D and height H could vary within certain limits, with typical values being ~2.5 and ~0.5 μm, respectively. In a case is no GaAs microlens

structure on the structure surface, the external quantum efficiency of the emitter η_{ext} is very low. Due to the total internal reflection (TIR) at the GaAs — air interface, and the critical angle of TIR for a given spectral range is ~16˚. The effect of TIR is significantly reduced with the use of GaAs microlens structure. The calculation of the η_{ext} depending on the GaAs microlens structure characteristics was performed by numerical solution of the Maxwell 3D equations. The calculation of the $\eta_{ext}(H)$ for a microlens with D= 2.4 μm shows that, as the lens curvature increases, the η_{ext} rises up from very low values and reaches the level of 20–25% for H ≥ 0.5 μm.

3. EXPERIMENTAL RESULTS

The structure containing $Al_xIn_{1-x}As$ QD's and (111)-oriented In(Ga)As QD's were studied by macrophotoluminescence and microphotoluminescence methods. The area of the excitation laser radiation spot at the structure surface was 3000 and 3 μm^2, respectively. The luminescence signal was excited with Nd:YAG laser radiation at the wavelength 532 nm in the continuous-wave (cw) mode of operation in a case of $Al_xIn_{1-x}As$ QD's structures and a tunable $Ti:Al_2O_3$ laser operating in the continuous regime as well as in the mode synchronization regime with a pulse duration of 3 ps in a case of (111)-oriented In(Ga)As QD's structures. The luminescence signal was detected with a single-grating monochromator equipped with a cooled Ge *p–i–n* photodiode (macroluminescence) or with a TriVista-555 triple-grating monochromator with a cooled CCD matrix of Si photodetectors (microluminescence). The luminescence peaks of single QDs were interpreted by applying the dependences of the intensities of the peaks on the excitation laser radiation power. At the lowest excitation powers, the exciton peaks X become evident in the luminescence spectra first, and the dependence of the intensities of these peaks on the excitation power is linear. At higher powers, biexciton peaks XX appear, whose intensity increases in accordance with a square law, as the laser power density is increased [18, 19]. The statistical properties of the emission of single QDs were studied with the use of a Hanbury Brown–Twiss (HBT) interferometer assembled in accordance with the classical scheme [18, 19]. Emission from the QD, when passed through the first TriVista-555 monochromator, was directed to a 50/50 CCM1-BS014 beam-splitting nonpolarizing prism that divided the incident light flux into strictly equal parts. Emission in each of the channels was recorded by photon counters based on PerkinElmer SPCM-AQRH-15 Si avalanche photodiodes; the time characteristics of emission were analyzed with a PicoHarp 300 coincidence counter.

The macrophotoluminescence spectra of structures containing $Al_xIn_{1-x}As$ /$Al_yGa_{1-y}As$ QD's with different compositions are shown in figure 1. The spectra were recorded at T= 295 K. The data demonstrate an extension of the spectral region of the emission of QD's to the short-wavelength region (to 200 nm), including the region close to 700 nm which is of interest for the engineering of atmospheric systems of quantum cryptography. The data shown in figure 1 were obtained for structure regions containing high density arrays of $Al_xIn_{1-x}As$ /$Al_yGa_{1-y}As$ QD's (with the density $d \geq 10^{10} cm^{-2}$). To study the characteristics of single QD's, we need low-density regions with $d \leq 10^8 cm^{-2}$. To solve this problem, we use an approach, in which the $Al_xIn_{1-x}As$ layer was grown without rotation of the substrate. This specified the gradient of the layer thickness; as a result, the structure contained QD regions with different densities in the range from zero to the maximum density $d \approx 10^{11} cm^{-2}$. The presence of areas with a low density of QD's on the synthesized structures allowed us to refer to single QD's and to study their optical characteristics by the microphotoluminescence technique. Figure 2 contains two microphotoluminescence spectra of the $Al_{0.1}In_{0.9}As/Al_{0.24}Ga_{0.76}As$ QD's structure, spectra were obtained for areas with different density of QD's. The bottom spectrum exhibits a narrow peak corresponding to recombination of the exciton X in a single $Al_{0.1}In_{0.9}As/Al_{0.24}Ga_{0.76}As$ QD. The statistics of emission of single QDs was analyzed by measuring pair photon correlations obtained with a HBT interferometer. Figure 3 shows the correlation function $g^2(\tau)$ determined for the exciton peak of a single $Al_{0.1}In_{0.9}As/Al_{0.24}Ga_{0.76}As$ QD (Figure 2, bottom spectrum). At $\tau = 0$, the dependence $g^2(\tau)$ has a well-pronounced minimum, $g^2(\tau) \approx 0.46$, which is indicative of the sub-Poisson type of emission statistics. This is direct verification of the possibility of producing single-photon emitters on the basis of $Al_{0.1}In_{0.9}As$ QDs.

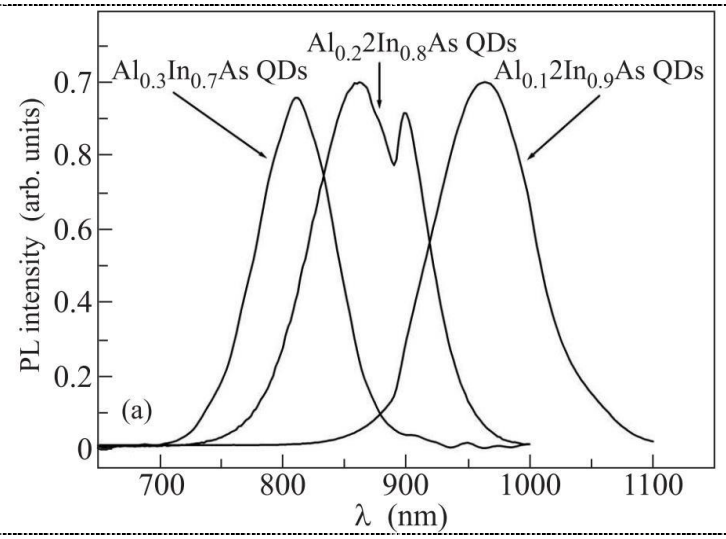

Figure 1. Photoluminescence spectra of three structures containing $Al_XIn_{1-X}As/Al_YGa_{1-Y}As$ QDs at T=295 K.

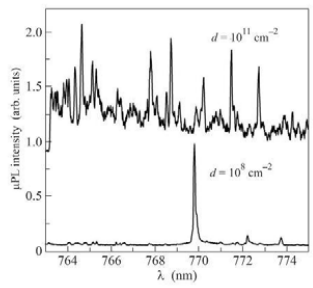

Figure 2. Microluminescence spectra for two regions of the $Al_{0.1}In_{0.9}As/Al_{0.24}Ga_{0.76}As$ structure with the QD density $d\approx10^{11}$ cm^{-2} (top) and $d=10^8 cm^{-2}$ (bottom) at T=10 K.

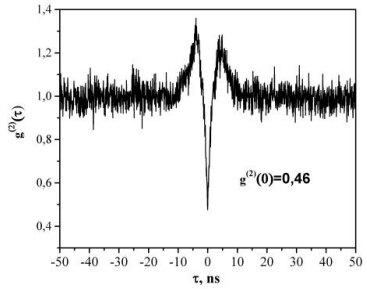

Figure 3. The second-order photon correlation function $g^2(\tau)$ for emission of a single $Al_{0.1}In_{0.9}As/Al_{0.24}Ga_{0.76}As$ QD, 770 nm spectral range, T=10 K.

The microphotoluminescence spectra of microlenses structures with single (111) In(Ga)As QD's are presented at Figure 4. Emission peaks of the only QD clearly manifest themselves in the microluminescence spectra of the completed microcavity structure with the microlens having a diameter of D= 2.4 μm and height of H=0.4μm. QD luminescence peaks were interpreted using the dependences of the peak intensities on the excitation-laser emission power. The peak of exciton X first and foremost manifests themselves at the lowest excitation powers in luminescence spectra, and power dependence of the intensity is linear. The peak of biexciton XX appear in the spectra at larger powers, the intensity of which increases according to quadratic law depending on the laser power density [13, 18]. In quantum optical measurements the second-order autocorrelation clearly reveals the single photon emission with $g^{(2)}(0) = 0.07$, (Figure 5).

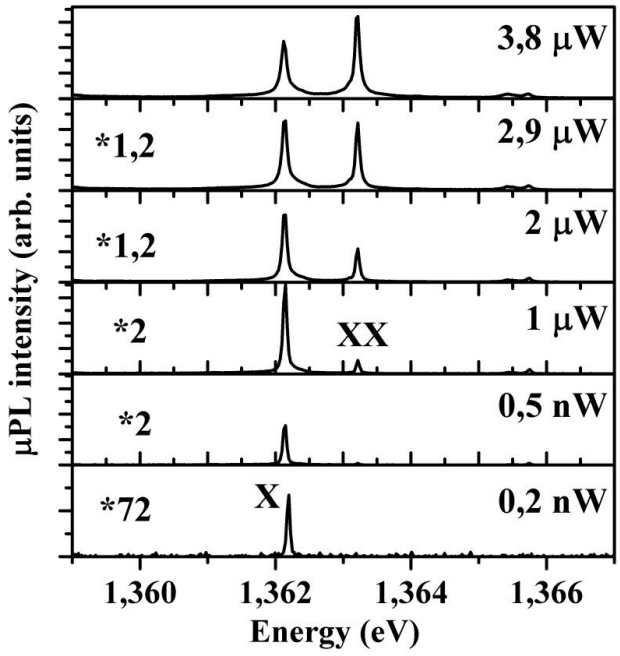

Figure 4. Microluminescence spectra of the structure based on deterministic microlens and (111) In(Ga)As QD's at different excitation powers at T=10 K.

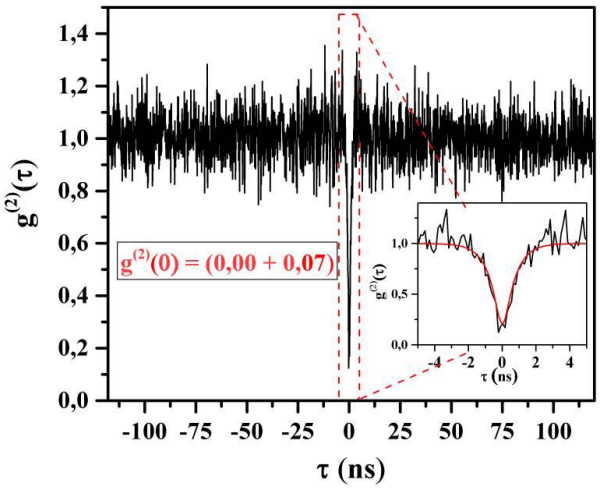

Figure 5. The second-order photon correlation function $g^2(\tau)$ for the structure based on deterministic microlens and single (111) In(Ga)As QD, measured at T=10 K.

4. CONCLUSIONS

Thus, in this study the systems of AlInAs- and (111) In(Ga)As-based QD's have been analyzed. The use of wide-gap $Al_xIn_{1-x}As$ alloys as a basis of QD's makes possible a substantial extension of the spectral region of emission to the short-wavelength region, including the region close to 770 nm which is of interest for the engineering of aerospace systems of quantum cryptography. The structures based on a bottom semiconductor Bragg reflector, top deterministic GaAs microlens structures and a single (111)

In(Ga)As QD shows a clear single – photon emission with a second – order correlation function at zero delay $g^{(2)}(0) = 0.07$. Both types of emitters are promising building block towards the realization of advanced quantum communication networks based on a single semiconductor QD.

This work has been partially supported by RFBR, Projects No. 16-52-12023.

REFERENCES

[1]. Knill E, Laflamme R, and Milburn G, 2001 Nature **46** 409
[2]. Kiraz A, Atatüre M, and Imamoğlu A 2004 Phys. Rev. A **69** 032305
[3]. Kok P, Munro W, Nemoto K, Ralph T, Dowling J, and Milburn G 2007 Rev. Mod. Phys.**79** 135
[4]. Gisin N and Thew R 2007 Nat. Photonics **1** 165
[5]. Kimble H 2008 Nature **453**, 1023
[6]. Michler P, Kiraz A, Becher C, Schoenfeld W, Petroff P, Zhang L, Hu E, and Imamoğlu A, 2000 Science **290** 2282
[7]. Santori C, Fattal D, Vučković J, Solomon G, and Yamamoto Y, 2002 Nature **419** 594.
[8]. Patel R, Bennett R, Cooper K, Atkinson P, Nicoll C, Ritchie D, and Shields A, 2008 Phys. Rev. Lett.**100** 207405
[9]. Ates S, Ulrich S, Ulhaq A, Reitzenstein S, Löffler A, Höfling S, Forchel A, and Michler P, 2009 Nat. Photonics **3** 724
[10]. Müller K, Rundquist A, Fischer K, Sarmiento T, Lagoudakis K, Kelaita Y, Sánchez Muñoz C, delValle E, Laussy F, and Vučković J,2015 Phys. Rev. Lett.**114** 233601.
[11]. Schliwa A, Winkelnkemper M, Lochmann A, Stock E, and Bimberg D 2009 Phys. Rev. B. **80** 161307
[12]. Bimberg D, Grundmann M and Ledentsov N 1999 *Quantum Dot Heterostructures* (Chichester: Wiley)
[13]. Michler P 2003 *Single Quantum Dots: Fundamentals, Applications and New Concepts* (Berlin: Springer)
[14]. Gisin N, Ribordy G, Tittel W, and Zbinden H, 2002 Rev. Mod. Phys. **74** 145
[15]. Li L, Chauvin N, Patriarche G, Alloing B, and Fiore A, 2008 J. Appl. Phys. **104** 08358
[16]. Krzyzewski T and Jones T,2004 J. Appl. Phys. **96** 668
[17]. Muller-Kirsch L, Heitz R, Pohl U, and Bimberg D, 2001 Appl. Phys. Lett. **79** 1027
[18]. Michler P 2009 *Single Semiconductor Quantum Dots* (Berlin: Springer)